Hard X-ray afterglows of short GRBs

Davide Lazzati*, Enrico Ramirez-Ruiz* and Gabriele Ghisellini†

*Institute of Astronomy, Madingley Road CB3 0HA Cambridge, U.K.
†Osservatorio Astronomico di Brera, via Bianchi 46, 23807 Merate (LC), Italy

Abstract. We report the discovery of a transient and fading hard X-ray emission in the BATSE lightcurves of a sample of short γ-ray bursts. We have summed each of the four channel BATSE light curves of 76 short bursts to uncover the average overall temporal and spectral evolution of a possible transient signal following the prompt flux. We found an excess emission peaking ~ 30 s after the prompt one, detectable for ≈ 100 s. The soft power-law spectrum and the time-evolution of this transient signal suggest that it is produced by the deceleration of a relativistic expanding source, as predicted by the afterglow model.

INTRODUCTION

Since their discovery, γ-ray bursts (GRBs) have been known predominantly as brief, intense flashes of high-energy radiation, despite intensive searches for transient signals at other wavelengths. Fortunately, the rapid follow-up of *Beppo*SAX [1] positions, combined with ground-based observations, has led to the detection of fading emission in X-rays [2], optical [3] and radio [4] wavelengths. These afterglows in turn enabled the measurement of redshifts [5], firmly establishing that GRBs are the most luminous known events in the Universe and involve the highest source expansion velocities.

The detection of afterglows that follow systematically long bursts has been a major breakthrough in GRB science. Unfortunately no observation of this kind was possible for short bursts. Our physical understanding of their properties was therefore put in abeyance, waiting for a new satellite better suited for their prompt localization.

In this paper we show that afterglow emission characterizes also the class of short bursts. In a comparative analysis of the BATSE lightcurves of 76 short bursts we detect a hard X-ray fading signal following the prompt emission with a delay of ~ 30 s. The spectral and temporal behavior of this emission is consistent with the one produced by a decelerating blast wave, providing a direct confirmation of relativistic source expansion. For a more detailed discussion, see Lazzati, Ramirez-Ruiz and Ghisellini [6].

DATA ANALYSIS

The detection of slowly variable emission in BATSE lightcurves is a non trivial issue, since BATSE is a non-imaging instrument and background subtraction can not be easily performed. We selected from the BATSE GRB catalog a sample of short duration ($T_{90} \leq 1$ s), high signal-to-noise ratio, GRB lightcurves with continuous data from ~ 120 s before the trigger to ~ 230 s afterwards. We aligned all the lightcurves to a common time reference in which the burst (binned to a time resolution of 64 ms) peaked at $t = 0$ and we binned the lightcurves in time by a factor 250, giving a time resolution of 16.0 s. The time bin $[-8 < t < 8$ s] containing the prompt emission was removed and the remaining background modelled with a 4^{th} degree polynomial. The bursts in which this fit yielded a reduced χ^2 larger than 2 in at least one of the four channels were discarded. Note that we did not subtract this best fit background curve from the data. This procedure was used only to reject lightcurves with very rapid and unpredictable background fluctuations and is based on the assumption that the excess burst or afterglow emission is not detectable in a single lightcurve. This procedure yielded a final sample of 76 lightcurves, characterized by an average duration $\langle T_{90} \rangle = 0.44$ s and fluence $\langle \mathcal{F} \rangle = 2.6 \times 10^{-6}$ erg cm^{-2}.

To search for excess emission following the prompt burst, we added the selected binned lightcurves in the four channels independently. The resulting lightcurves are shown in the upper panels of Fig. 1 by the solid points. Error bars are computed by propagating the Poisson uncertainties of the individual lightcurves.

The lightcurves in the third and fourth channels can be successfully fitted with polynomials. The third (110–

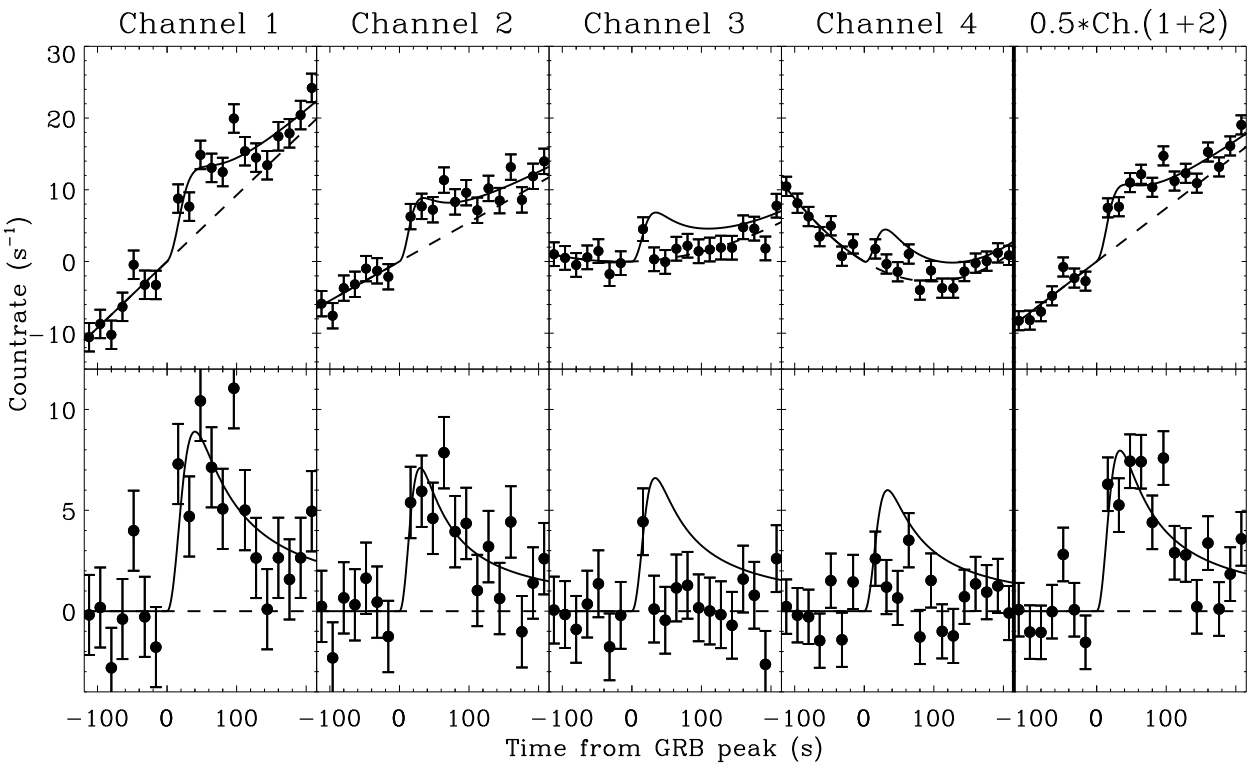

FIGURE 1. Overall lightcurves in the 4 BATSE channels (from left to right) of the sample of short bursts (see text). The rightmost panels show the average signal in the first and second channels. The time interval of the burst emission has been excluded. The upper panels show the lightcurves without background subtraction (a constant has been subtracted in all panels for viewing purposes in order to have zero counts at $t = 0$). The solid line is the best fit background plus afterglow model (in the channel 3 and 4 panels the 3σ upper limit afterglow is shown). The dashed line shows the background contribution in all channels. The lower panels show the same data and fit after background subtraction.

325 keV) and fourth (> 325 keV) channel lightcurves can be fitted with a quadratic model, yielding $\chi^2/\text{d.o.f.} = 17/18$ and $\chi^2/\text{d.o.f.} = 18.5/17$ respectively. In the first two channels, a polynomial model alone does not give a good description of the data. In the first (25–60 keV) channel, a cubic fit yields $\chi^2/\text{d.o.f.} = 42/16$, while in the second (60–110 keV) we obtain $\chi^2/\text{d.o.f.} = 26/16$. A more accurate modelling of the first two channels lightcurves can be achieved by allowing for an afterglow emission following the prompt burst. We model the afterglow lightcurve with a smoothly joined broken power-law function:

$$L_A(t) = \frac{3L_A}{\left(\frac{t_A}{t}\right)^2 + \frac{2t}{t_A}}; \quad t > 0 \qquad (1)$$

which rises as t^2 up to a maximum L_A that is reached at time t_A and then decays as t^{-1}. Adding this afterglow component to the fit, we obtain $\chi^2/\text{d.o.f.} = 28.5/16$ and $14.7/16$ in the first and second channels, respectively. The χ^2 variation, according to the F-test, is significant to the $\sim 3.5\sigma$ level in both channels. The fact that the fit in the first channel is only marginally acceptable should not surprise. This is because the excess is due to many afterglow components peaking at different times, and has therefore a more "symmetric" shape than Eq. 1. A fully acceptable fit can be obtained with a different shape of the excess, but we used the afterglow function for simplicity. By adding together the first two channels, the afterglow component is significant at the 4.2σ level. The results of the fit are reported in Tab. 1.

TABLE 1. Fit results. Quoted errors at 90% levels, upper limits at 3σ level.

	E (keV)	L_A (cts s^{-1})	t_A (s)
Channel #1	[25-60]	8.9 ± 2.6	40 ± 16
Channel #2	[60-110]	7.1 ± 2.4	30^{+16}_{-10}
Channel #1+2	[25-110]	16 ± 3.5	33.5^{+24}_{-15}
Channel #3	[110-325]	< 6.6	33.5 (fixed)
Channel #4	> 325	< 6.0	33.5 (fixed)

DISCUSSION

In order to understand whether the excess is residual prompt burst emission or afterglow emission, we computed its four channel spectrum. To convert BATSE count rates to fluxes, we computed an average response matrix for our burst sample by averaging the matrices of single bursts obtained from the `discsc_bfits` and `discsc_drm` datasets. The resulting spectrum is shown in Fig. 2. The dark points show the spectrum at $t = 30$ s (the peak of the afterglow in the second BATSE channel), which is consistent with a single power-law $F(\nu) \propto \nu^{-1}$ (black dashed line). Grey points show the time integrated spectrum (fluences has been measured with a growth curve technique), consistent with a steeper power-law $F(\nu) \propto \nu^{-1.5}$ (grey dashed line). These power-law spectra are much softer than any observed burst spectrum (independent of their duration). This spectral diversity, together with the fact that a single power-law does not fit the data, suggest that the emission is not due to a tail of burst emission but more likely to an early hard X-ray afterglow. This also confirms earlier predictions that the mechanism responsible for the afterglow emission is different from that of the prompt radiation.

An interesting comparison can be made with the early afterglow of long GRBs. Connaughton [7] finds that on average the BATSE countrate is ~ 150 cts s^{-1} at $t = 50$ s after the main event. In our short GRB sample, the countrate at the same time is ~ 15 cts s^{-1}. Since the luminosity of the average early X-ray afterglow is representative of the total isotropic energy of the fireball, we can conclude that the isotropic equivalent energy of the short bursts is on average ten times smaller than that of the long ones (or that their true energy is the same, but the jet opening angle is three times larger). Indeed, the γ-ray fluence of long bursts is on average ten times larger than that of short bursts.

In the case of short bursts, the analysis of the afterglow emission is made easier by the lack of superposition with the prompt burst flux. For this reason the time and luminosity of the afterglow peak can be directly measured while in long bursts it had to be inferred from the shape of the decay law at longer times. In our case, however, the lightcurve in Fig. 1 is the result of the sum of many afterglow lightcurves, with different peak times and luminosities. For a given isotropic equivalent energy E, afterglows peaking earlier (with larger Γ) are expected to be brighter and should dominate the composite lightcurve. On the other hand, for a given Lorentz factor Γ, afterglow peaking earlier (with lower E) are dimmer. The fact that the ~ 35 s timescale is preserved, suggests that there are only few very energetic bursts with a large bulk Lorentz factor.

We must also remain aware of other possibilities. For instance, we may be wrong in assuming that the central object goes dormant after producing the initial explosion. A sudden burst followed by a slowly decaying energy input could arise if the newly formed black hole slowly swallows the orbiting torus around it or if the central object becomes a rapidly-spinning pulsar rather than a black hole. This luminosity may dominate the continuum afterglow at early times before the blast wave decelerates. Under this interpretation, the hard X-ray transient following the prompt emission could be attributed to the central object itself rather than to a standard decelerating blast wave. Contrary to what is observed, this emission should smoothly decay after the main episode, unless this energy is converted into a relativistic outflow which is in turn converted to radiation at a larger radius.

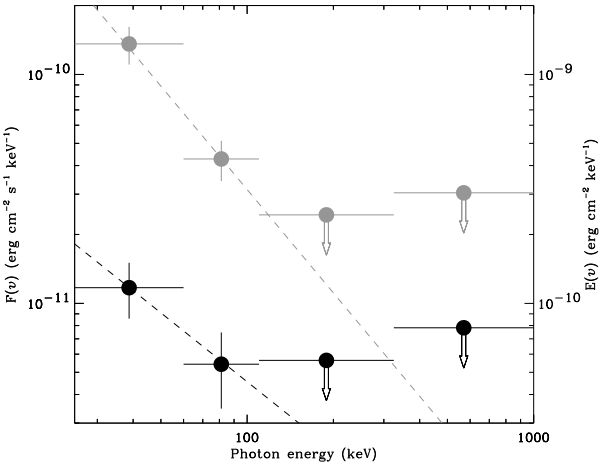

FIGURE 2. Spectrum of the peak afterglow emission. Black dots (and left vertical axis) show the spectrum at $t = 30$ s. Gray dots (right vertical axis) show the time integrated spectrum as obtained from the four BATSE channel counts. Error bars are for 90% uncertainties, while arrows are 3σ upper limits.

REFERENCES

1. Boella, G., Butler, R. C., Perola, G. C., Piro, L., Scarsi, L., and Bleeker, J. A. M., *A&AS*, **122**, 299–307 (1997).
2. Costa, E. e. a., *Nature*, **387**, 783–785 (1997).
3. van Paradijs, J. e. a., *Nature*, **386**, 686–689 (1997).
4. Frail, D. A., Kulkarni, S. R., Nicastro, S. R., Feroci, M., and Taylor, G. B., *Nature*, **389**, 261–263 (1997).
5. Metzger, M. R., Djorgovski, S. G., Kulkarni, S. R., Steidel, C. C., Adelberger, K. L., Frail, D. A., Costa, E., and Frontera, F., *Nature*, **387**, 878–880 (1997).
6. Lazzati, D., Ramirez-Ruiz, E., and Ghisellini, G., *A&A*, **379**, L39–L43 (2001).
7. Connaughton, V., *ApJ in press (astro-ph/0111564)* (2001).